Simulation-Based Inference of KiDS-1000 Cosmic Shear

Maximilian von Wietersheim-Kramsta

www.wietersheim-kramsta.com
maximilian.wietersheim-kramsta.19@ucl.ac.uk

12/03/2024 - Imperial College London

Kiyam Lin

Nicolas Tessore

Benjamin Joachimi

Arthur Loureiro

Robert Reischke

Angus Wright

Challenges facing galaxy surveys

- Galaxy surveys are getting **wider**, **deeper** and **more precise**.

  $\Rightarrow$ Galaxy clustering and weak lensing probes become sensitive to **non-linear scales**

  $\Rightarrow$ The S/N becomes high enough that **higher-order statistics** can be measured precisely

  $\Rightarrow$ Observational **systematics** begin limiting the precision

$\Rightarrow$ "Traditional" signal and noise modelling can become inaccurate/too expensive.

Simulation-Based Inference (SBI)

A.k.a. *likelihood-free* or *implicit likelihood inference*

- Signal and noise modelling as complex as simulations can be.
- Likelihood can take an arbitrary form (non-Gaussian).
- Full Bayesian uncertainty propagation from measurements to parameters.
- Number of simulations required similar to the number needed for numerical covariances [Lin et al. 2022; arxiv:2212.04521].

SBI: Approximate Bayesian Computation

$$P(\boldsymbol{\theta}|\boldsymbol{d}) = \frac{P(\boldsymbol{d}|\boldsymbol{\theta}) \cdot P(\boldsymbol{\theta})}{P(\boldsymbol{d})} \tag{1}$$

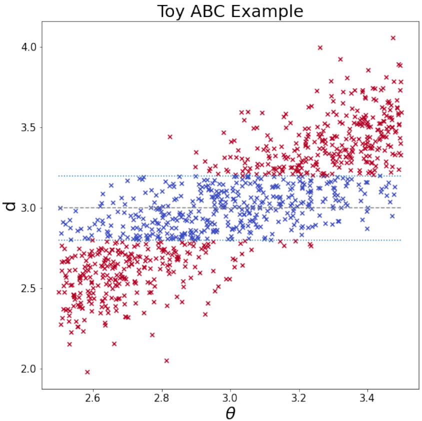

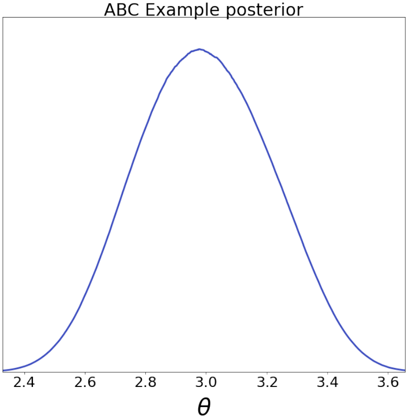

SBI: Density Estimation

$$P(\theta|\boldsymbol{d}) = \frac{P(\boldsymbol{d}|\theta) \cdot P(\theta)}{P(\boldsymbol{d})} \propto P(\boldsymbol{\theta}, \boldsymbol{d}) \cdot P(\boldsymbol{\theta}) \quad (2)$$

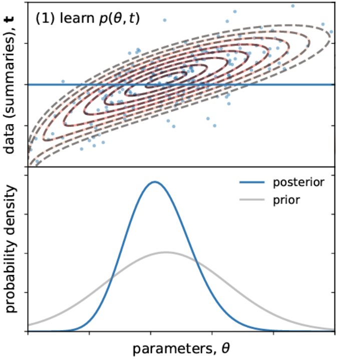

Figure: [Alsing et al. 2019]

Kilo-Degree Survey: KiDS-1000

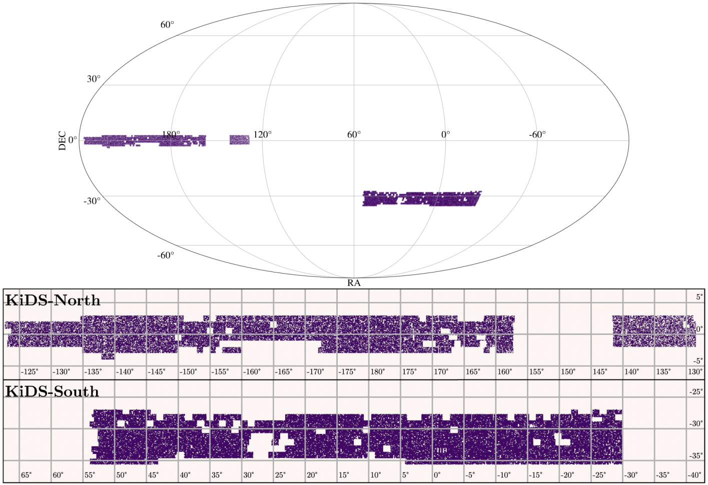

Previous KiDS-1000 Cosmic Shear Results

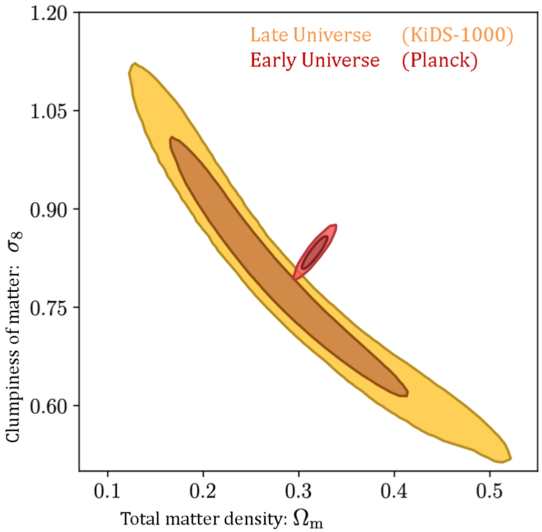

Requirements for Cosmic Shear Forward-Simulations

- Physically accurate
  - Require highly resolved matter and shear fields
  - Consideration of relevant systematic effects: baryonic feedback and intrinsic alignments
- Realistic
  - Consideration of survey characteristics
  - Choice of data vector
- Fast
  - Many realisations required for DELFI
- Expandable
  - Future-proof implementations

Forward-Simulation Pipeline

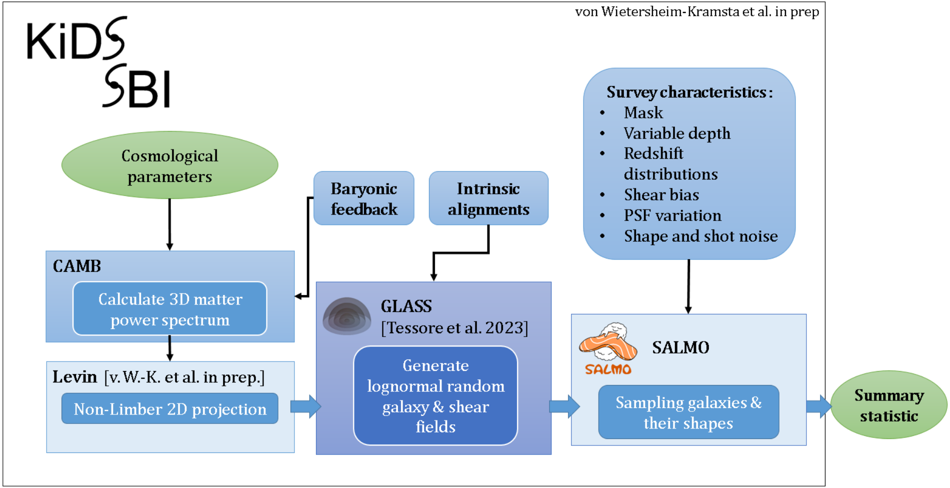

Geometry of the simulations

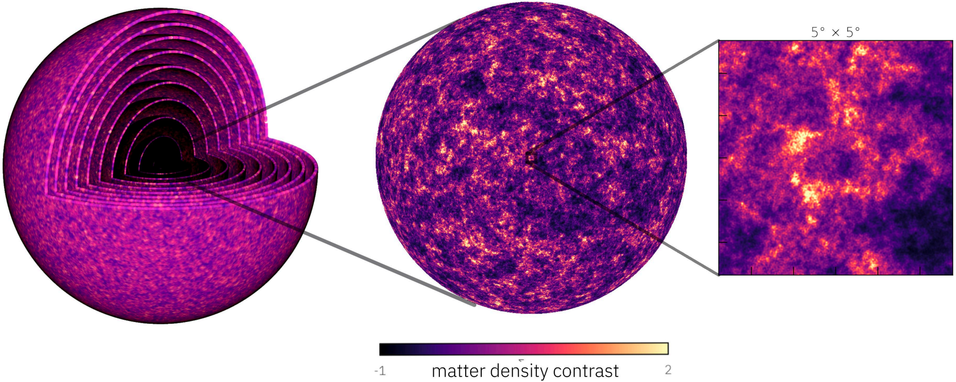

Figure: [Tessore et al. 2023; arxiv:2302.01942]

Geometry of the simulations

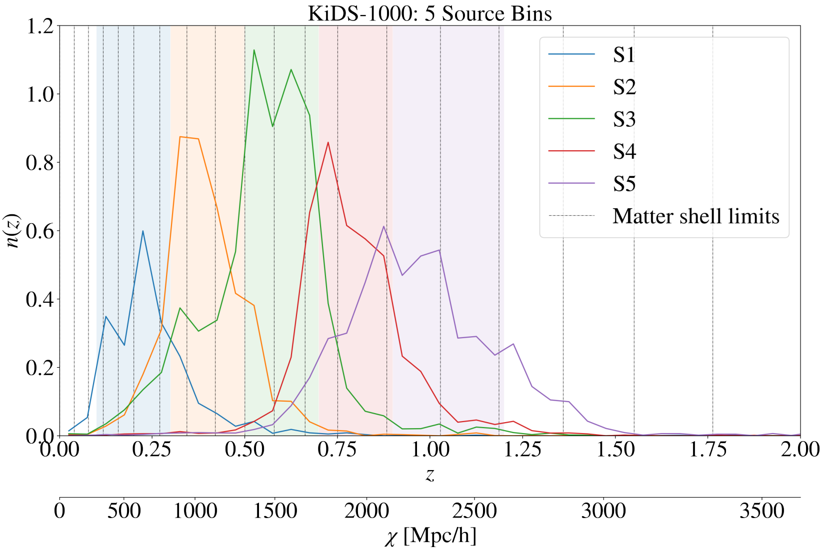

Non-Limber Projection: Levin

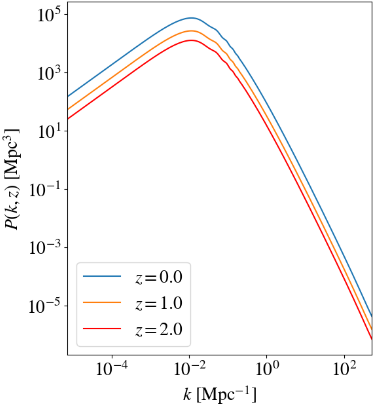

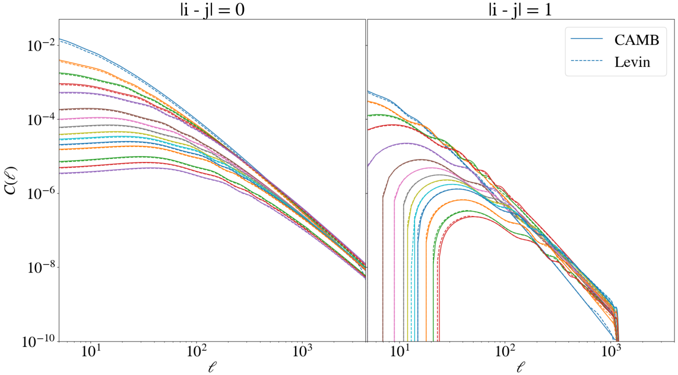

GLASS: Generator of Large Scale Structure

$$C_{\delta\delta}^{(ij)}(\theta; \mathbf{\Theta}) = \langle \delta^{(i)}(\theta; \mathbf{\Theta}) \, \delta^{(j)*}(\theta; \mathbf{\Theta}) \rangle \tag{3}$$

$$\kappa(\theta, z; \mathbf{\Theta}) = \frac{3\Omega_m}{2} \int_0^z \mathrm{d}z' \, \frac{f_k(z'; \mathbf{\Theta}) \, (f_k(z'; \mathbf{\Theta}) - f_k(z; \mathbf{\Theta}))}{f_k(z; \mathbf{\Theta})} \frac{1 + z'}{E(z'; \mathbf{\Theta})} \, \delta(\theta, z'; \mathbf{\Theta}), \tag{4}$$

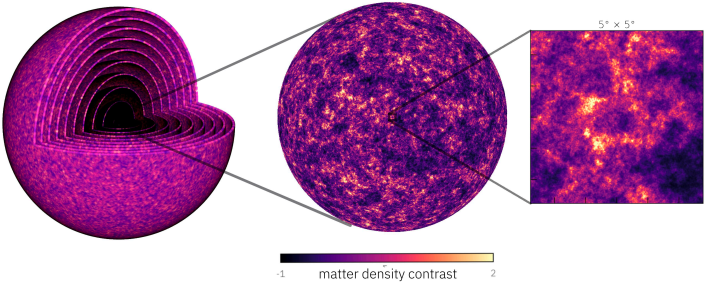

Intrinsic Alignments: Field-level NLA model

$$\kappa^{(i)}(\theta_m;\boldsymbol{\Theta}) \to \kappa^{(i)}(\theta_m;\boldsymbol{\Theta}) + \kappa^{(i)}_{\rm IA}(\theta_m;\boldsymbol{\Theta}). \tag{5}$$

$$\kappa^{(i)}_{\rm IA}(\theta_m;\boldsymbol{\Theta}) = -A_{\rm IA}\,\frac{C_1\,\Omega_{\rm m}\,\overline{\rho}_{\rm cr}(\overline{z}^{(i)};\boldsymbol{\Theta})}{D(\overline{z}^{(i)};\boldsymbol{\Theta})}\,\delta^{(i)}(\theta_m;\boldsymbol{\Theta}), \tag{6}$$

For a given matter shell:

Lensing convergence (κ) +
IA convergence (κ_{IA}) from NLA

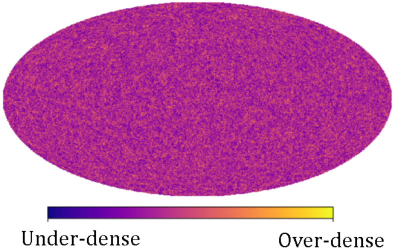

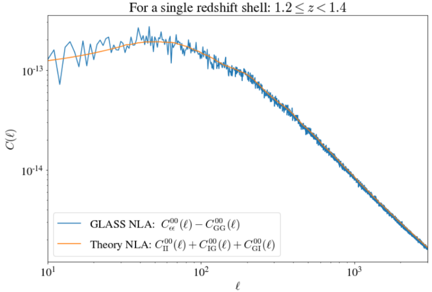

Survey Characteristics

Shell Tomographic bin

$$\langle N_m^{(i)(p)} \rangle(\boldsymbol{\Theta}) = w_m(\Omega_{\mathrm{survey}}) \left[1 + b^{(i)} \delta^{(i)}(\theta_m; \boldsymbol{\Theta})\right] P_m(p|i)\, n_{\mathrm{gal},m}^{(p)} A_{\mathrm{pix},m}$$

Pixel

Mask

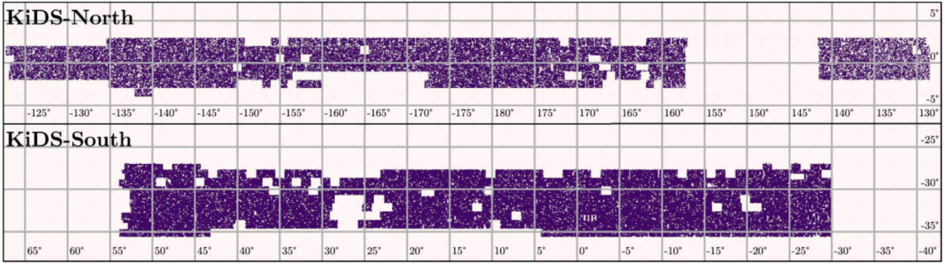

Survey Characteristics

Shell

Tomographic bin

$$\langle N_m^{(i)(p)} \rangle(\boldsymbol{\Theta}) = w_m(\Omega_{\mathrm{survey}}) \left[1 + b^{(i)} \delta^{(i)}(\theta_m; \boldsymbol{\Theta}) \right] P_m(p|i)\, n_{\mathrm{gal},m}^{(p)}\, A_{\mathrm{pix},m}$$

Pixel

Redshift distributions

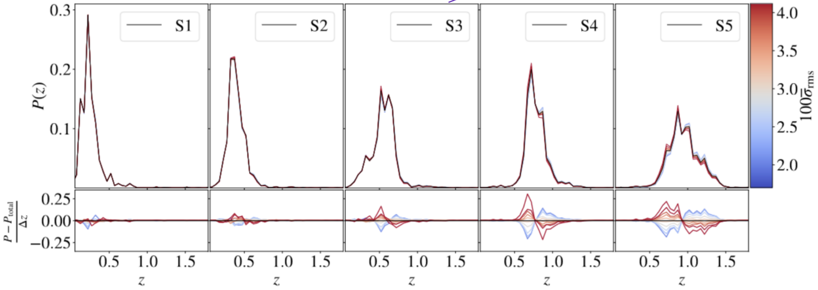

Survey Characteristics

Shell

Tomographic bin

$$\langle N_m^{(i)(p)} \rangle(\boldsymbol{\Theta}) = w_m(\Omega_{\rm survey}) \left[1 + b^{(i)} \delta^{(i)}(\theta_m; \boldsymbol{\Theta})\right] P_m(p|i)\, n_{{\rm gal},m}^{(p)}\, A_{{\rm pix},m}$$

Pixel

Galaxy density (variable depth)

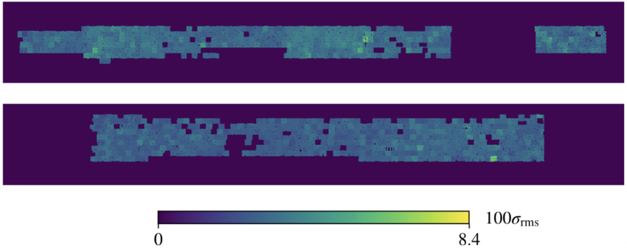

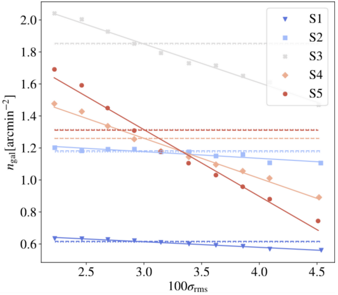

Variable Depth

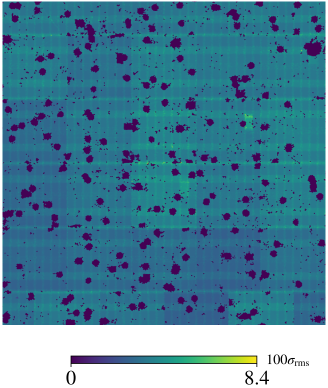

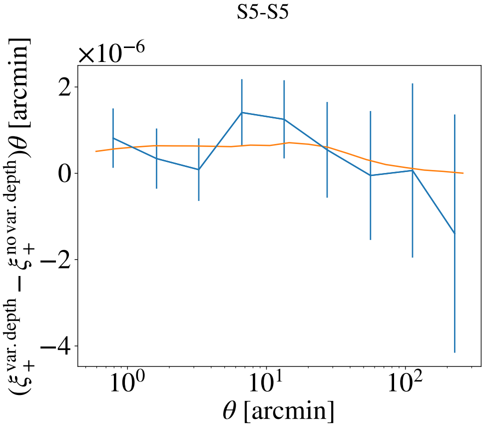

Figure: Orange: theory [Heydenreich et al. 2020; arXiv:1910.11327]. Blue: forward-simulations.

Survey Characteristics

Reduced shear

$$\epsilon_{\text{lensed}}(\boldsymbol{\Theta}) = \frac{\epsilon_{\text{int}} + g(\boldsymbol{\Theta})}{1 + g^*(\boldsymbol{\Theta})\epsilon_{\text{int}}}$$

Intrinsic shapes
(variable depth)

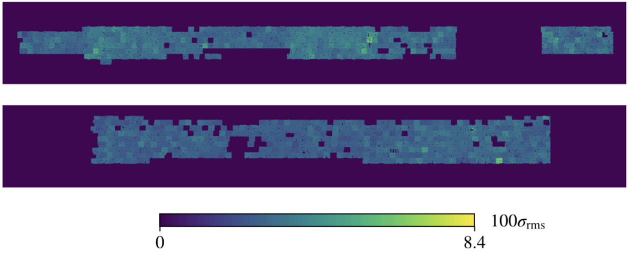

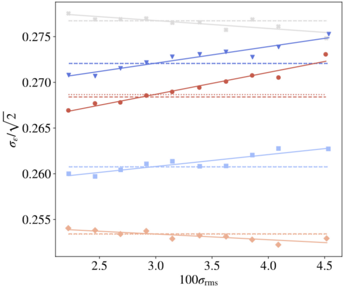

Survey Characteristics

$$\epsilon_{\mathrm{obs}}(p, m; \mathbf{\Theta}) = \left(1 + M^{(p)}\right)\epsilon_{\mathrm{lensed}}(\mathbf{\Theta}) + \alpha^{(p)}\epsilon_{\mathrm{PSF}}(m) + \cancel{\beta^{(p)}\delta\epsilon_{\mathrm{PSF}}} + c^{(p)}$$

Pixel

0

Tomographic bin

Multiplicative shear bias

PSF shear bias

Additive shear bias

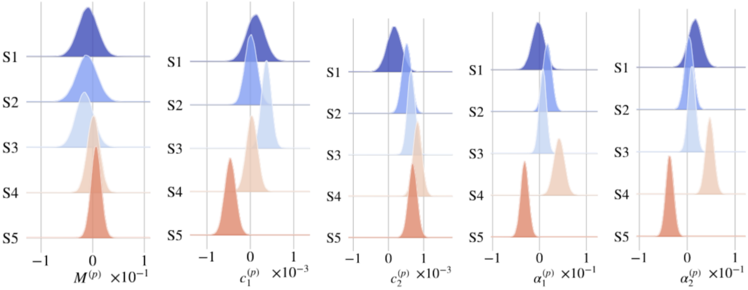

Survey Characteristics

Pixel

$$\epsilon_{\mathrm{obs}}(\boldsymbol{p}, \boldsymbol{m}; \boldsymbol{\Theta}) = \left(1 + M^{(\boldsymbol{p})}\right)\epsilon_{\mathrm{lensed}}(\boldsymbol{\Theta}) + \alpha^{(\boldsymbol{p})}\epsilon_{\mathrm{PSF}}(\boldsymbol{m}) + \cancelto{0}{\beta^{(\boldsymbol{p})}\delta\epsilon_{\mathrm{PSF}}} + c^{(\boldsymbol{p})}$$

Tomographic bin

PSF shear bias

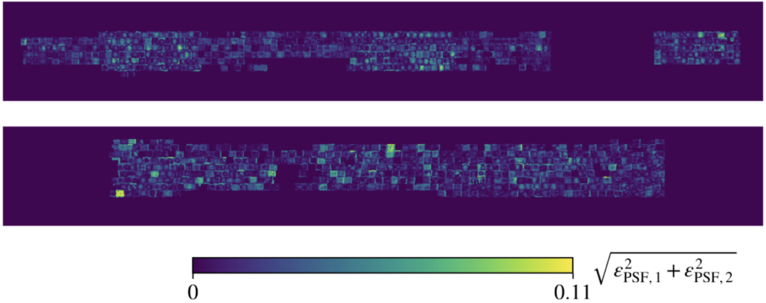

Measurement: Pseudo-Cls

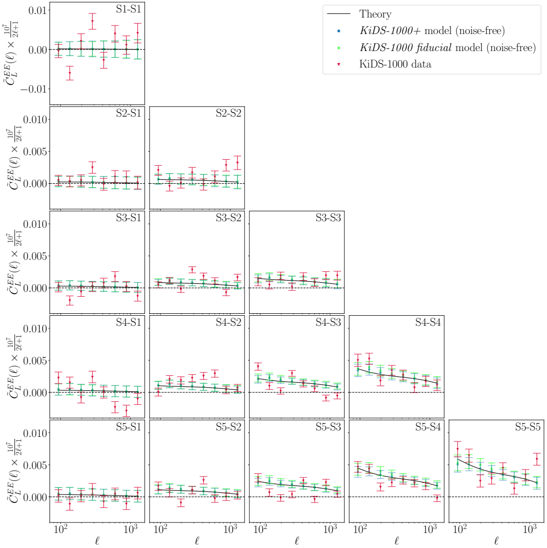

Forward-simulations speed

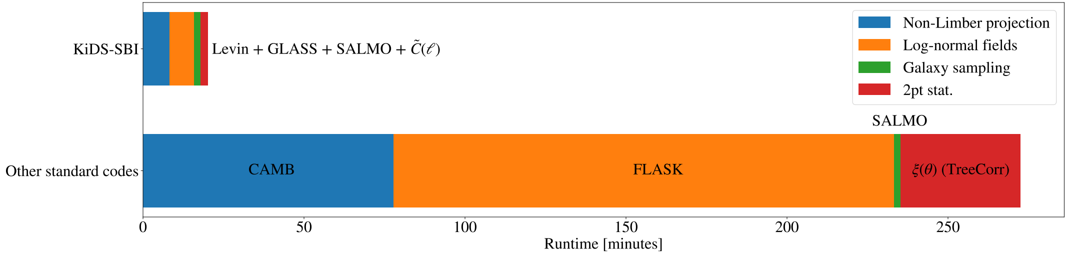

KiDS-SBI

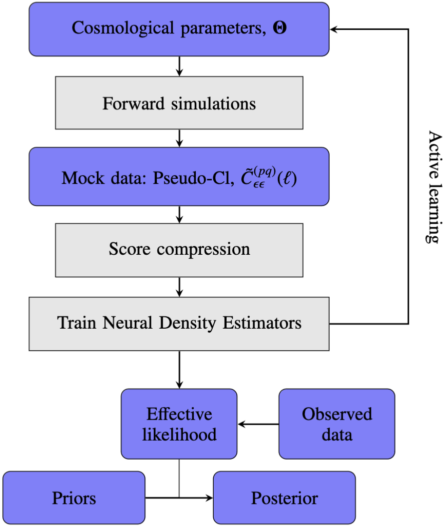

Cosmological parameters, $\boldsymbol{\Theta}$
Forward simulations
Mock data: Pseudo-Cl, $\tilde{C}_{\epsilon\epsilon}^{(pq)}(\ell)$
Score compression
Train Neural Density Estimators
Active learning
Effective likelihood
Observed data
Priors
Posterior

KiDS-SBI: Parameters and Priors

Parameter	Symbol	Prior type	Prior range	Fiducial
Density fluctuation amp.	S_8	Flat	[0.1, 1.3]	0.76
Hubble constant	h_0	Flat	[0.64, 0.82]	0.767
Cold dark matter density	ω_{c}	Flat	[0.051, 0.255]	0.118
Baryonic matter density	ω_{b}	Flat	[0.019, 0.026]	0.026
Scalar spectral index	n_{s}	Flat	[0.84, 1.1]	0.901
Intrinsic alignment amp.	A_{IA}	Flat	[-6, 6]	0.264
Baryon feedback amp.	A_{bary}	Flat	[2, 3.13]	3.1
Redshift displacement	$\boldsymbol{\delta}_z$	Gaussian	$\mathcal{N}(\mathbf{0}, \boldsymbol{C}_z)$	$\mathbf{0}$
Multiplicative shear bias	$M^{(p)}$	Gaussian	$\mathcal{N}(\overline{M}^{(p)}, \sigma_M^{(p)})$	$\overline{M}^{(p)}$
Additive shear bias	$c_{1,2}^{(p)}$	Gaussian	$\mathcal{N}(\overline{c}_{1,2}^{(p)}, \sigma_{c_{1,2}}^{(p)})$	$\overline{c}_{1,2}^{(p)}$
PSF variation shear bias	$\alpha_{1,2}^{(p)}$	Gaussian	$\mathcal{N}(\overline{\alpha}_{1,2}^{(p)}, \sigma_{\alpha_{1,2}}^{(p)})$	$\overline{\alpha}_{1,2}^{(p)}$

Internal Consistency

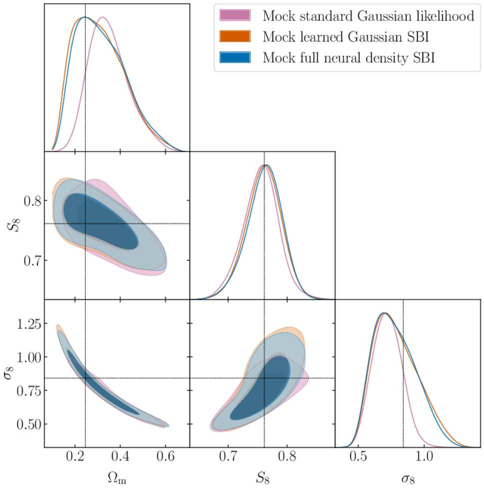

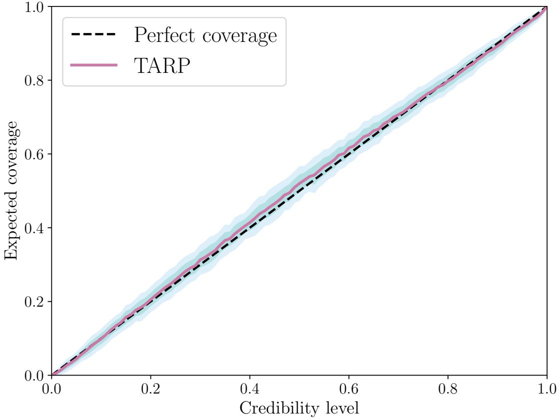

Goodness-of-Fit in SBI

$$\chi^2(\boldsymbol{t}|\boldsymbol{\Theta}) = (\boldsymbol{t}_i - \mathrm{E}[\boldsymbol{t}_*|\boldsymbol{\Theta}_*])^{\mathrm{T}}(\mathrm{Cov}(\boldsymbol{t}_*|\boldsymbol{\Theta}_*))^{-1}(\boldsymbol{t}_i - \mathrm{E}[\boldsymbol{t}_*|\boldsymbol{\Theta}_*]) \tag{7}$$

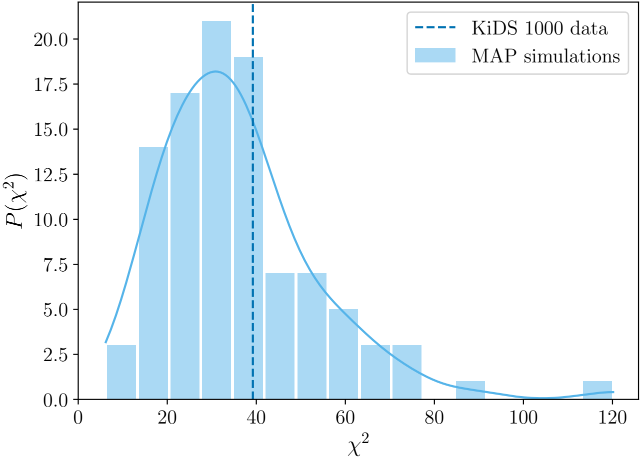

Posterior Probability

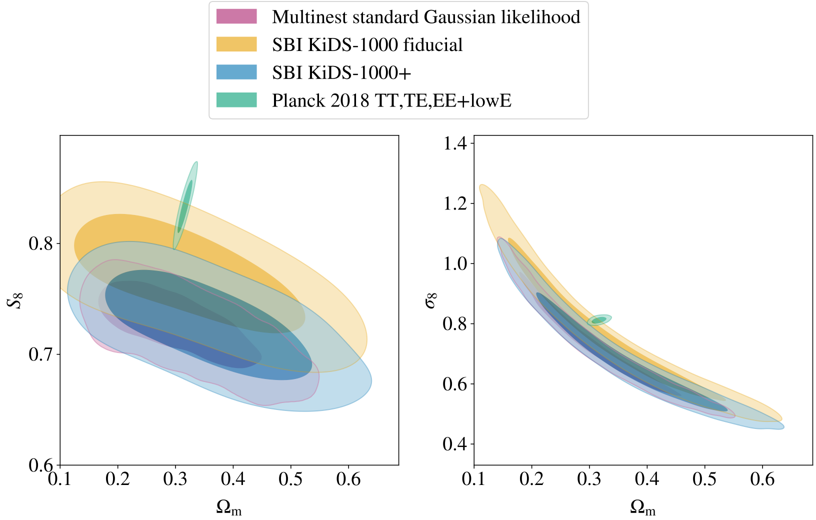

Posterior Probability

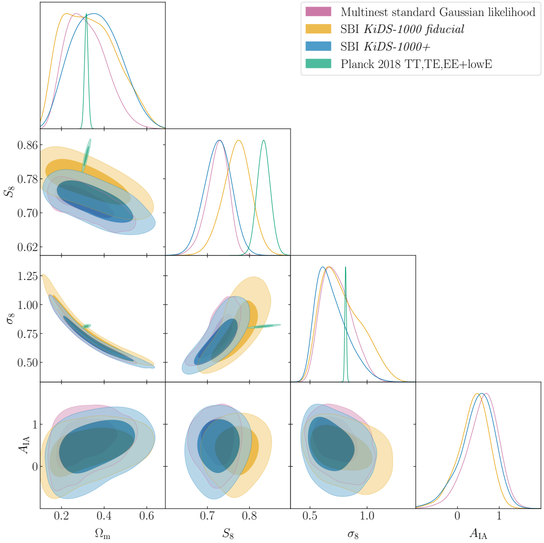

S_8-dependent Uncertainty

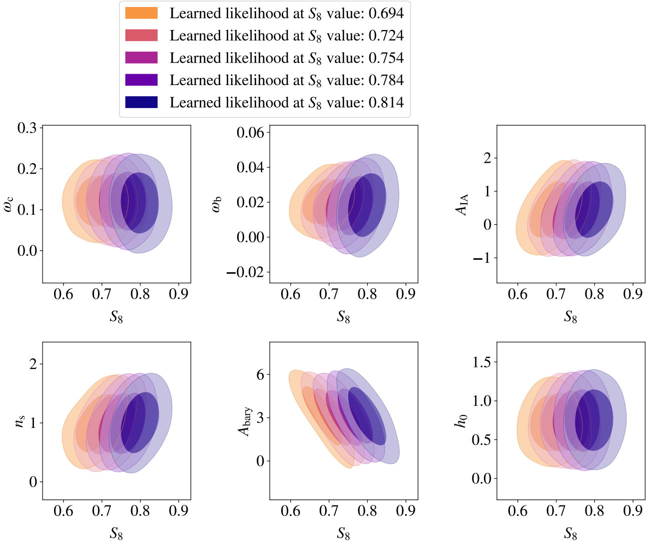

S_8-dependent Uncertainty from Theory

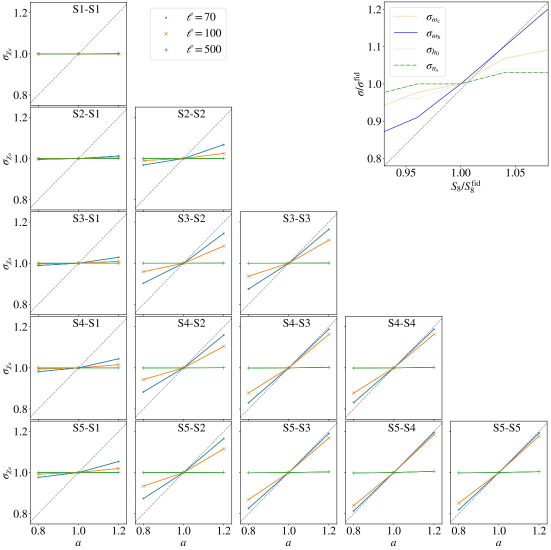

KiDS-SBI: Conclusions

- Neglecting variable depth and shear biases can bias S_8 by approx. 5%
- Cosmic shear likelihood is consistent with a Gaussian, but its covariance is measurably cosmology-dependent (cosmic variance) $\rightarrow$ uncertainty on S_8 is higher
- **Future**: test different models, apply to 3x2pt analysis, analyse KiDS-Legacy or Euclid, etc.

Questions?

References

Niall Jeffrey, Justin Alsing, François Lanusse (2020)
Likelihood-free inference with neural compression of DES SV weak lensing map statistics
MNRAS Volume 501, Issue 1, February 2021, Pages 954–969.

Nicolas Tessore, et al. (in prep.)

Arthur Loureiro, et al. (2021)
KiDS & Euclid: Cosmological implications of a pseudo angular power spectrum analysis of KiDS-1000 cosmic shear tomography
arxiv 2110.06947v1 .

David Levin (1994)
Fast integration of rapidly oscillatory functions
JCAM Volume 67, Issue 1, 20 February 1996, Pages 95-101.

References

Justin Alsing et al. (2019)
Fast likelihood-free cosmology with neural density estimators and active learning
Monthly Notices of the Royal Astronomical Society Volume 488, Issue 3, September 2019, Pages 4440-4458.

Justin Alsing et al. (2018)
Massive optimal data compression and density estimation for scalable, likelihood-free inference in cosmology
Monthly Notices of the Royal Astronomical Society Volume 477, Issue 3, July 2018, Pages 2874–2885.

Appendices A - Pipeline Setup

- Shear-shear weak lensing from KiDS-1000 using pseudo-Cls
- Latin hypercube of cosmology values as simulation input

Parameter	Symbol	Prior type	Prior range	Fiducial
Density fluctuation amp.	S_8	Flat	[0.1, 1.3]	0.76
Hubble constant	h_0	Flat	[0.64, 0.82]	0.767
Cold dark matter density	ω_c	Flat	[0.051, 0.255]	0.118
Baryonic matter density	ω_b	Flat	[0.019, 0.026]	0.026
Scalar spectral index	n_s	Flat	[0.84, 1.1]	0.901
Intrinsic alignment amp.	A_{IA}	Flat	[-6, 6]	0.264
Baryon feedback amp.	A_{bary}	Flat	[2, 3.13]	3.1
Redshift displacement	$\boldsymbol{\delta}_z$	Gaussian	$\mathcal{N}(\mathbf{0}, \boldsymbol{C}_z)$	$\mathbf{0}$
Multiplicative shear bias	$M^{(p)}$	Gaussian	$\mathcal{N}(\overline{M}^{(p)}, \sigma_M^{(p)})$	$\overline{M}^{(p)}$
Additive shear bias	$c_{1,2}^{(p)}$	Gaussian	$\mathcal{N}(\overline{c}_{1,2}^{(p)}, \sigma_{c_{1,2}}^{(p)})$	$\overline{c}_{1,2}^{(p)}$
PSF variation shear bias	$\alpha_{1,2}^{(p)}$	Gaussian	$\mathcal{N}(\overline{\alpha}_{1,2}^{(p)}, \sigma_{\alpha_{1,2}}^{(p)})$	$\overline{\alpha}_{1,2}^{(p)}$

Appendices B - Compression and DELFI

- A stack of NDEs are used in DELFI

$$p(\mathbf{t}|\theta;\mathbf{w}) = \prod_{\alpha=1}^{N_{\mathrm{NDEs}}} \beta_\alpha p_\alpha(\mathbf{t}|\theta;\mathbf{w}), \tag{8}$$

- A mixture of Gaussian Mixture Density Networks (MDNs) and Masked Autoregressive Flows (MAFs) are employed in this ensemble
- Further massive compression from summary statistics to reduce dimensionality via score compression

$$\mathcal{L} = \mathcal{L}_* + \delta\boldsymbol{\theta}^T \nabla\mathcal{L}_* - \frac{1}{2}\delta\boldsymbol{\theta}^T \mathbf{J}_* \delta\boldsymbol{\theta}, \tag{9}$$

$$\boldsymbol{t} = \nabla\boldsymbol{\mu}^T \boldsymbol{C}^{-1}(\boldsymbol{d} - \boldsymbol{\mu}), \tag{10}$$

- Remap this to a MLE estimate via the Fisher matrix

$$\hat{\theta} = \theta_* + \boldsymbol{F}_*^{-1}\nabla\mathcal{L}_* = \theta_* + \boldsymbol{F}_*^{-1}\boldsymbol{t}_*, \tag{11}$$

Appendices C - PyDELFI

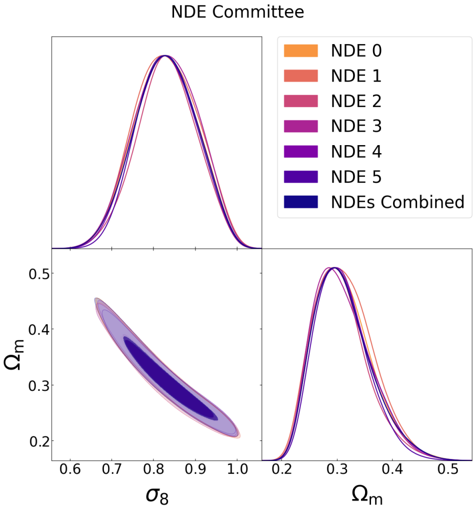

[Alsing et al. 2019]

Appendices D - SBI - ABC

$$P(\boldsymbol{\theta}|\boldsymbol{d}) = \frac{P(\boldsymbol{d}|\boldsymbol{\theta}) \cdot P(\boldsymbol{\theta})}{P(\boldsymbol{d})} \tag{12}$$

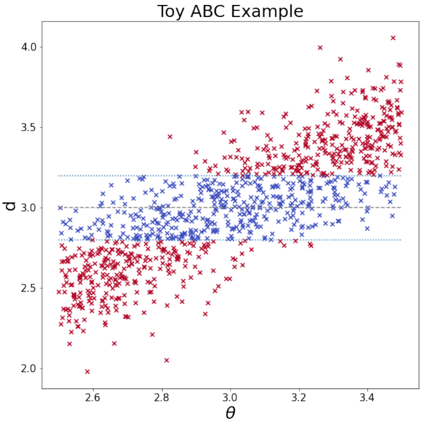

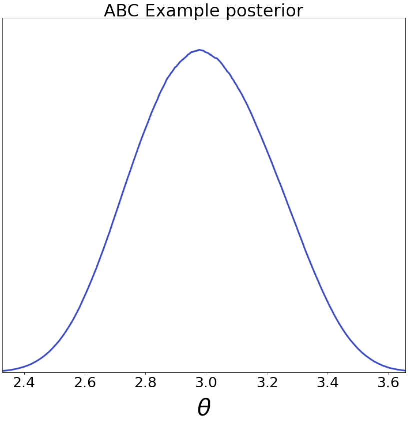

Appendices E - Score Compression

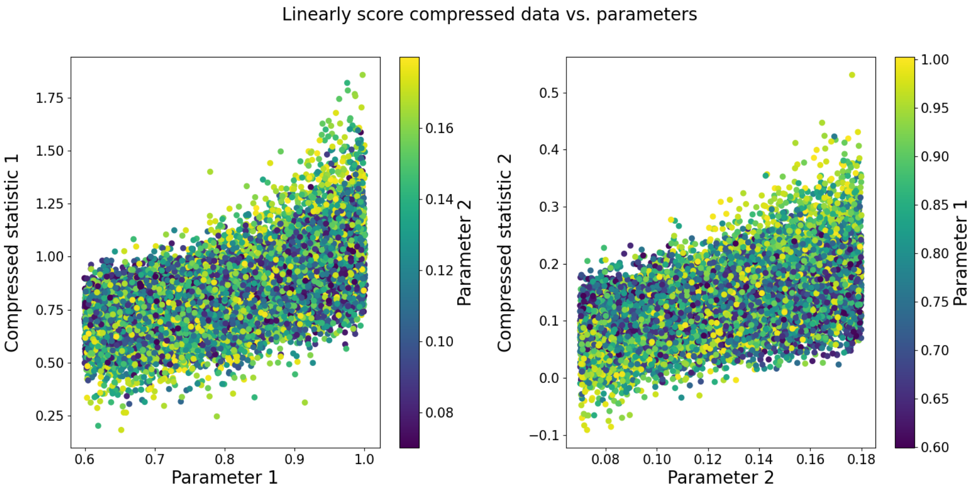

[Alsing et al. 2018]

$$\mathbf{t} = \mathbf{M}(\mathbf{d})$$

Appendices F - Sensitivity to Compression

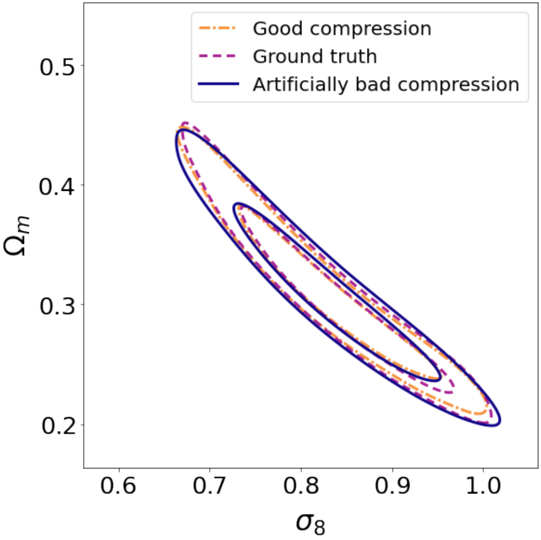

Appendix G - Sensitivity to Fiducial Cosmology

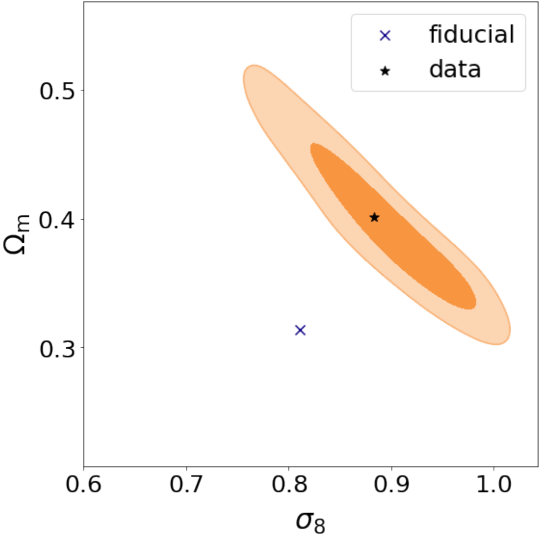

Appendix H - Active Learning

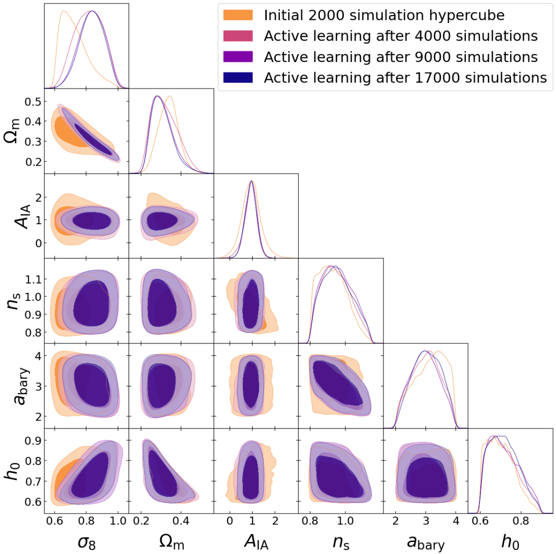

Appendix I - Simulation Number Sufficiency

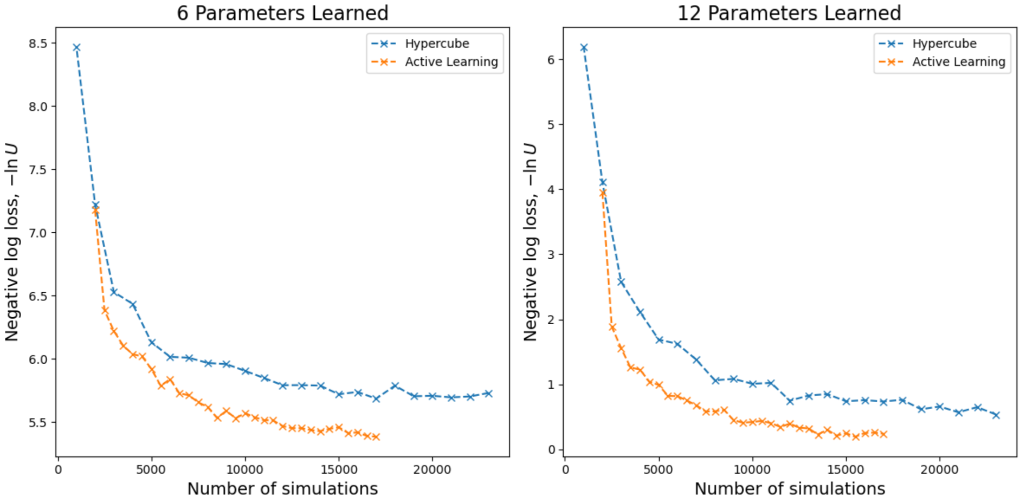

Appendix J - Full Posterior

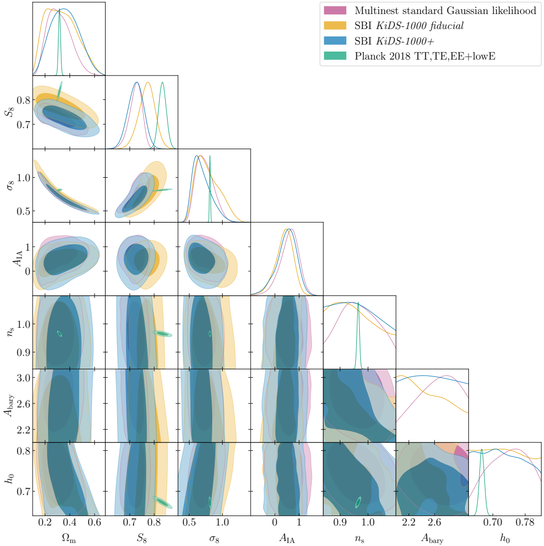

Appendix K - Signal Test